Dentomaxillofacial Radiology (2015) 44, 20150079

birpublications.org/dmfr

RESEARCH ARTICLE

# 3D dento-maxillary osteolytic lesion and active contour segmentation pilot study in CBCT: semi-automatic *vs* manual methods

[1,2,3]K Vallaeys, [2,4,5]A Kacem, [1,3]H Legoux, [1,3]M Le Tenier, [2,4]C Hamitouche and [1,2,3]R Arbab-Chirani

*[1]UFR d'Odontologie, Université de Bretagne Occidentale, Brest, France; [2]Laboratoire de Traitement de l'Information Médicale, LaTim-Inserm UMR 1101, Brest, France; [3]Service d'Odontologie, Centre Hospitalier Régional Universitaire Brest, France; [4]Départment Image et Traitement de l'Information, Telecom Bretagne, Brest, France; [5]Institut National des Sciences Appliquées et de Technologies de Tunis, INSAT, Tunis, Tunisia*

**Objectives:** This study was designed to evaluate the reliability of a semi-automatic segmentation tool for dento-maxillary osteolytic image analysis compared with manually defined segmentation in CBCT scans.
**Methods:** Five CBCT scans were selected from patients for whom periapical radiolucency images were available. All images were obtained using a ProMax® 3D Mid Planmeca (Planmeca Oy, Helsinki, Finland) and were acquired with 200-μm voxel size. Two clinicians performed the manual segmentations. Four operators applied three different semi-automatic procedures. The volumes of the lesions were measured. An analysis of dispersion was made for each procedure and each case. An ANOVA was used to evaluate the operator effect. Non-paired *t*-tests were used to compare semi-automatic procedures with the manual procedure. Statistical significance was set at $\alpha = 0.01$.
**Results:** The coefficients of variation for the manual procedure were 2.5–3.5% on average. There was no statistical difference between the two operators. The results of manual procedures can be used as a reference. For the semi-automatic procedures, the dispersion around the mean can be elevated depending on the operator and case. ANOVA revealed significant differences between the operators for the three techniques according to cases.
**Conclusions:** Region-based segmentation was only comparable with the manual procedure for delineating a circumscribed osteolytic dento-maxillary lesion. The semi-automatic segmentations tested are interesting but are limited to complex surface structures. A methodology that combines the strengths of both methods could be of interest and should be tested. The improvement in the image analysis that is possible through the segmentation procedure and CBCT image quality could be of value.
*Dentomaxillofacial Radiology* (2015) **44**, 20150079. doi: 10.1259/dmfr.20150079

**Cite this article as:** Vallaeys K, Kacem A, Legoux H, Le Tenier M, Hamitouche C, Arbab-Chirani R. 3D dento-maxillary osteolytic lesion and active contour segmentation pilot study in CBCT: semi-automatic *vs* manual methods. *Dentomaxillofac Radiol* 2015; **44**: 20150079.

Correspondence to: Dr Karen Vallaeys. E-mail: karen.vallaeys@univ-brest.fr

The present study has contributed to testing some semi-automatic segmentation protocols on dento-maxillary imaging. To our knowledge, no studies have yet been carried out on CBCT and odontogenic cysts. Region-based active contour segmentation was comparable with the manual procedure for delineating circumscribed osteolytic dento-maxillary lesions. However, region-based and boundary-based segmentation are not suitable for all cases. These approaches are limited when segmenting objects with complex surface structures. A hybrid methodology, combining the strength of both manual and semi-automatic protocols, needs to be developed in order to provide a suitable method for the majority of cases, regardless of clinical situation, extent and position of the lesion. The improvement of the image analysis must be considered through the segmentation procedure and CBCT image quality.

This work was partly supported by the French ANR within the Investissements d'Avenir programme (LabEx CAMI) under reference ANR-11-LABX-004.
Received 7 March 2015; revised 15 May 2015; accepted 20 May 2015

**Keywords:** CBCT; dento-maxillary osteolytic image; jaw cysts; 3D dento-maxillary imaging; image segmentation

## Introduction

The use of CBCT is increasing in dento-maxillofacial practice. CBCT can be beneficial in dento-maxillofacial imaging and can be considered as the present reference technique.[1–3] CBCT has a high resolution and causes lower radiation exposure compared with multislice CT (MSCT). CBCT enables the clinician to obtain linear

**Table 1** CBCT periapical index scores (Estrela et al[7])

| *Score* | *Quantitative bone alterations in mineral structures* |
|---|---|
| 0 | Intact periapical bone structures |
| 1 | Diameter of periapical radiolucency >0.5–1 mm |
| 2 | Diameter of periapical radiolucency >1–2 mm |
| 3 | Diameter of periapical radiolucency >2–4 mm |
| 4 | Diameter of periapical radiolucency >4–8 mm |
| 5 | Diameter of periapical radiolucency >8 mm |
| Score (n) +E | Expansion of periapical cortical bone |
| Score (n) +D | Destruction of periapical cortical bone |

measurements of anatomic structures and lesions in the maxillary and mandibular bones on three planes of space and is considered to be accurate *in vivo* and *in vitro*.[4–6] It can give accurate volumetric and linear measurements that are of interest for monitoring treatment outcomes and patient follow-up during the healing phase. Several studies have been published confirming the high accuracy of CBCT for diagnosing periapical lesions and radiolucency.[4,7]

In the field of dento-maxillary osteolytic images, radicular cysts are the main diagnosis for jaw cysts and cyst-like lesions of the mandible, accounting for >50% of cases.[8] Most non-healing lesions submitted for biopsy are classified as granulomas or cysts (73% of cases).[9] Radicular cysts are inflammatory disorders of the periradicular tissues, caused by persistent microbial infection of the root canal system of the affected teeth. The prevalence of periapical radiolucency is very high, broadly equivalent to one radiolucency per patient.[10] These pathoses cause bone resorption and may generate extensive tissue destruction that requires surgical intervention. Maxillary approaches require surgeons to drill the bone to expose target lesions while avoiding the critical structures within it, such as the neurovascular bundle, maxillary sinus or nasal fossa. Indeed, a misguided action may create damage causing permanent injury, paraesthesia etc. An understanding and an evaluation of the anatomical specificities of individual patients are important to develop a case-specific risk assessment. In complex cases when surgery is planned, a planning and guidance support

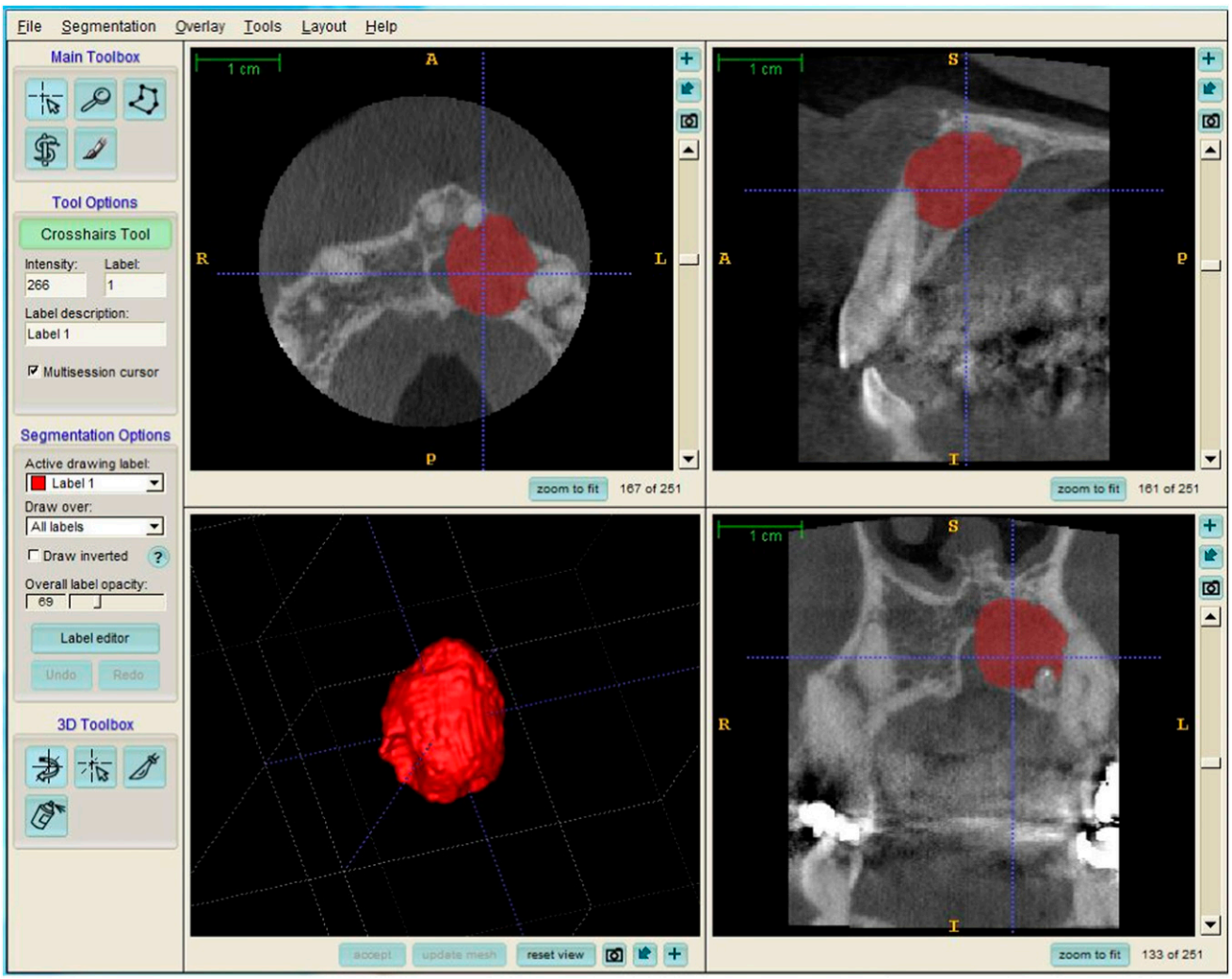


**Figure 1** Example of manual segmentation result. A, anterior; I, inferior; L, left; P, posterior; R, right; S, superior.

**Table 2** Operator effect, ANOVA $\alpha = 0.01$

| *Case* | *MAN* | *EB* | *RC* | *EBDA* |
|---|---|---|---|---|
| 1 | 0.189 | 0.0119 | 0.126 | <0.0001* |
| 2 | 0.373 | <0.0001* | 0.771 | 0.0007* |
| 3 | 0.668 | 0.063 | <0.0001* | 0.0226 |
| 4 | 0.772 | <0.0001* | <0.0001* | 0.0031* |
| 5 | 0.028 | 0.599 | 0.335 | 0.0094* |

EB, semi-automatic procedure with edge-based contour evolution; EBDA, semi-automatic procedure with edge-based contour evolution by adjunction of an anisotropic diffusion filter; MAN, manual procedure; RC, semi-automatic procedure with region competition contour evolution.
*Statistically significant difference.

system would be beneficial. Three-dimensional (3D) representation of pathological structures must be very accurate to be suitable for virtual planning, highlighting its relation with the surrounding anatomical structures, especially with the critical areas of the inferior alveolar dental nerve in the mandible, the maxillary sinus and nasal cavities.[11] Some studies have proposed and validated a method for estimating preoperative and postoperative bone volume using CBCT imaging *in vitro*.[12] Presently, there is no standardized method clinically usable *in vivo*.

The first step of preparation for surgical planning and bone volume evaluation is tissue segmentation. This needs to be performed as quickly as possible with as few user interactions as possible and an accurate result. Voxels are gathered according to certain criteria that make it possible to isolate images within the structures that need to be analysed. Accurate segmentation of the CBCT image is an essential step for generating 3D models for the diagnosis and treatment planning of patients with voluminous osteolytic disease. This is a critical step because it affects the quality of subsequent measurement and analyses. Inaccurate information may lead to mistakes of measurement and treatment simulation. The difficulty of segmentation lies in the variation of the target structure, which differs according to the clinical case. Several segmentation techniques exist: manual, semi-automatic and fully automatic.

The most straightforward approach to segmentation is the manual method, where the user outlines the structures slice by slice. By defining a region of interest (ROI) in each slice, a volume of interest can be composed after combining all successive ROIs. Manual segmentation is often used as a reference compared with all automated segmentation procedures, but manual segmentation is very time consuming and user dependent.[13]

In complex images, automatic methods lead to inaccuracies that often require the operator to correct the results,[13] which is one reason why semi-automatic methods are of interest. They combine the efficiency and repeatability of automatic segmentation with the sound judgment that can only come from human expertise.[14] Many semi-automatic segmentation protocols have been described in the literature. Among these, two active contour segmentation methods have become well-established theoretical approaches: Geodesic Active Contours and Region Competition.[15,16] The human expert must specify the initial contour, balance the various forces that act upon it and monitor the evolution of the segmentation. Semi-automatic segmentation methods greatly assist the clinician in this task.

ITK-SNAP (Penn Image Computing and Science Laboratory, Philadelphia, PA), an open source medical image processing application, implements these two methods. This software application provides a combination of manual and semi-automatic tools for extracting structures in 3D image data of different modalities and from different anatomical regions.[14]

The purpose of this study was to compare semi-automatic segmentation methods for CBCT scans with manual segmentation for dento-maxillary osteolytic 3D image reconstruction and analyses.

## Methods and materials

### *Study sample*

For this study, a total of five CBCT data sets of patients, presenting a periapical radiolucent image with a CBCT periapical index score from 4 to 5 ED (expansion and destruction of periapical bone; see Table 1), were selected. This index was developed on the basis of criteria established from measurements corresponding to periapical radiolucency interpreted on CBCT scans (Table 1).[7] All the images have been anonymized.

### *CBCT imaging protocol, data acquisition and data export*

All the CBCT image data sets were obtained using ProMax® 3D Mid Planmeca X-ray source equipment (Planmeca OY, Helsinki, Finland). The data sets were obtained for diagnosis and before treatment of the patients. All data sets were acquired with a 200-μm isotropic voxel size, *i.e.* with a $0.2 \times 0.2 \times 0.2$ mm spatial resolution, two fields of view ($7 \times 5$ or $4 \times 5$ cm), a tube (anode) voltage of 90 kV and a tube (anode) current of 11–13 mA. The image detector was a flat panel.

**Table 3** Manual procedure, statistical data

| *Case* | *1* | | *2* | | *3* | | *4* | | *5* | |
|---|---|---|---|---|---|---|---|---|---|---|
| *Operator* | *A* | *B* | *A* | *B* | *A* | *B* | *A* | *B* | *A* | *B* |
| Mean volume ($mm^3$) | 428.95 | 437.68 | 1651.90 | 1620.04 | 871.00 | 877.79 | 406.40 | 408.94 | 116.49 | 135.33 |
| Median volume ($mm^3$) | 427.78 | 438.66 | 1630.17 | 1619.36 | 881.79 | 879.15 | 404.57 | 405.16 | 112.94 | 134.55 |
| Standard deviation | 9.30 | 2.27 | 53.46 | 13.43 | 19.83 | 15.99 | 11.12 | 8.85 | 6.20 | 7.47 |
| CV (%) | 2.17 | 0.52 | 3.24 | 0.83 | 2.28 | 1.82 | 2.74 | 2.16 | 5.32 | 5.52 |

CV, coefficient of variation.

**Table 4** Region competition procedure, statistical data

| *Case* | *1* | | | | *2* | | | | *3* | | | | *4* | | | | *5* | | | |
|---|---|---|---|---|---|---|---|---|---|---|---|---|---|---|---|---|---|---|---|---|
| *Operator* | *A* | *B* | *C* | *D* | *A* | *B* | *C* | *D* | *A* | *B* | *C* | *D* | *A* | *B* | *C* | *D* | *A* | *B* | *C* | *D* |
| Mean ($mm^3$) | 442.77 | 458.75 | 516.87 | 393.41 | 1668.84 | 1626.72 | 1678.72 | 1624.88 | 1345.80 | 1277.31 | 1128.00 | 974.17 | 456.86 | 614.74 | 467.84 | 278.96 | 135.38 | 139.49 | 171.50 | 139.69 |
| Standard deviation | 17.41 | 24.26 | 145.62 | 35.77 | 78.22 | 85.37 | 147.78 | 80.04 | 76.36 | 138.85 | 50.99 | 101.51 | 55.79 | 70.84 | 62.24 | 37.42 | 26.20 | 31.05 | 31.41 | 44.52 |
| CV (%) | 3.93 | 5.29 | 28.17 | 9.09 | 4.69 | 5.25 | 8.80 | 4.93 | 5.67 | 10.87 | 4.52 | 10.42 | 12.21 | 11.52 | 13.30 | 13.41 | 19.35 | 22.26 | 18.31 | 31.87 |

CV, coefficient of variation.

Image acquisition was performed in a standing position by a single 360° rotation with a variable scanning time (18–26 s pulsed X-ray). The number of slices (images) in each set was 251. The acquisition time ranged from 12.252 to 12.312 ms. All available data sets were exported in digital imaging and communications in medicine format.

*Segmentation protocol*

The method selected for the segmentation procedures used ITK-SNAP software (Penn Image Computing and Science Laboratory).[11,14,17] This software is an open source medical image processing application that provides a combination of manual and semi-automatic tools for extracting structures in 3D image data of different modalities and from different anatomical regions.[14] It was developed based on the library of image analysis algorithms, Insight ToolKit, and the library of visualization algorithms and advanced modelling techniques, Visualization ToolKit.

*Manual volumetric segmentation*

Two clinicians experienced in endodontics and dental imaging performed the manual segmentations (MAN, Operators A and B). The data were segmented twice to verify the variability of the manual segmentation.

Manual segmentation was performed with the open source software ITK-SNAP v. 2.4.0.[18] Every case ($n = 5$) was segmented manually using slice-by-slice boundary drawing in all three orthogonal views. This procedure was performed three times for each case at a minimum time interval of 2 weeks. The time spent by the two operators ranged from 1 to 3 h depending on the case. The manual segmentations performed served as the gold standard (Figure 1).

*Semi-automated segmentation*

Semi-automatic segmentations were performed using the same software mentioned above. Three different procedures were applied. The first two methods were developed and proposed by ITK-SNAP. The procedures use 3D active contour methods to compute feature images based on the CBCT image grey level intensity and boundaries. The principle of active contours is to evolve an initialized curve towards the outlined object of interest. The first method forces the active contour to slow down near edges, or discontinuities, of intensity (edge-based contour evolution or EB). The second method causes the active contour to be attracted to boundaries of regions of uniform intensity and to reach equilibrium (region competition contour evolution or RC).[14] The third method was developed from edge-based contour evolution by adjunction of an anisotropic diffusion filter (EBDA).

Four operators applied the protocol: three dental clinicians experienced in endodontics and dental imaging and an engineer experienced in image analysis. It was performed five times for each case with an interval of 2 weeks between the same procedures. Two operators performed both manual and semi-automatic procedures.

**Table 5** Edge-based procedure, statistical data

| *Case* | *1* | | | | *2* | | | | *3* | | | | *4* | | | | *5* | | | |
|---|---|---|---|---|---|---|---|---|---|---|---|---|---|---|---|---|---|---|---|---|
| *Operator* | *A* | *B* | *C* | *D* | *A* | *B* | *C* | *D* | *A* | *B* | *C* | *D* | *A* | *B* | *C* | *D* | *A* | *B* | *C* | *D* |
| Mean ($mm^3$) | 433.39 | 479.94 | 473.04 | 381.82 | 1708.81 | 1799.69 | 1670.17 | 1570.69 | 1077.99 | 1124.20 | 1084.17 | 1011.03 | 484.41 | 579.23 | 359.91 | 358.77 | 132.47 | 127.83 | 106.74 | 149.57 |
| Standard deviation | 9.36 | 20.34 | 41.34 | 76.45 | 31.27 | 57.32 | 39.59 | 60.47 | 75.55 | 89.79 | 44.66 | 61.50 | 60.42 | 81.85 | 21.75 | 53.31 | 48.98 | 21.78 | 77.90 | 27.01 |
| CV (%) | 2.16 | 4.24 | 8.74 | 20.02 | 1.83 | 3.19 | 2.37 | 3.85 | 7.01 | 7.99 | 4.12 | 6.08 | 12.47 | 14.13 | 6.04 | 14.86 | 36.98 | 17.04 | 72.98 | 18.06 |

CV, coefficient of variation.

The operators selected the best parameters according to the case and to the method.

The segmentation results were visualized by a 3D display of the segmented structures. Once the procedure had been finished, the software provided the volume of the segmented structure ($mm^3$). The volumes of the lesion 3D reconstructions were used to provide statistics. Time spent was less than 10 min for all operators. All the results were classified according to the case, the technique and the operator.

*Statistical methods*

All data were analysed using StatView v. 5.0 (SAS Institute Inc., Cary, NC). The accuracy of different approaches was calculated by comparing the volumes ($mm^3$) obtained by semi-automatic with manual segmentation. For each protocol and each case, an analysis of dispersion among-operator and within-operator sum of squares (mean, standard deviation and coefficient of variation) was made. An ANOVA test was used to evaluate the operator effect. An *a posteriori* Bonferroni–Dunn test was also applied if a statistically significant difference was previously noticed, to determine which means differ. Non-paired *t*-tests were used to compare semi-automatic with manual procedures. Statistical significance was set at $\alpha = 0.01$. The null hypothesis was that there was no significant difference in lesion volume measurement between the semi-automatic methods and the manual delineation.

## Results

*Manual protocol*

The coefficient of variation for the manual protocol ranged from 0.5% to 5.5% with a mean of 2.5–3.5% within operator. The correlation coefficient between the operators was 0.9997. There was no statistically significant difference between the two operators, for each pair, by ANOVA 1%. The results of the manual segmentation protocol can therefore be used as a reference (Tables 2 and 3).

*Semi-automatic protocol*

The coefficients of variation for the semi-automatic protocol were quite high for Case 4 and especially for Case 5, meaning that the dispersion around the mean can be high, depending on the operator (Tables 4–6).

*Operator effect*

The ANOVA analysis showed significant differences among the operators, for the edge-based technique, regarding Case 2 and 4 segmentations. The *post hoc* test (Bonferroni–Dunn) showed a significant difference between Operators A and D, B and C, B and D and C and D for Case 2; and A and C, A and D, B and C and B and D for Case 4.

There were significant differences among operators for the region competition procedure in Cases 3 and 4 (ANOVA). With the *post hoc* test, there were significant

**Table 6** Edge-based with an anisotropic diffusion, statistical data

| *Case* | *1* | | | | *2* | | | | *3* | | | | *4* | | | | *5* | | | |
|---|---|---|---|---|---|---|---|---|---|---|---|---|---|---|---|---|---|---|---|---|
| *Operator* | *A* | *B* | *C* | *D* | *A* | *B* | *C* | *D* | *A* | *B* | *C* | *D* | *A* | *B* | *C* | *D* | *A* | *B* | *C* | *D* |
| Mean ($mm^3$) | 481.84 | 560.42 | 635.54 | 435.60 | 1776.46 | 1838.38 | 1825.97 | 1572.32 | 1116.14 | 1245.48 | 1183.96 | 1118.78 | 539.24 | 674.08 | 369.58 | 346.30 | 110.02 | 126.96 | 207.86 | 133.68 |
| Standard deviation | 25.66 | 43.17 | 53.39 | 6.20 | 76.79 | 40.71 | 73.52 | 135.58 | 43.14 | 85.63 | 75.42 | 55.80 | 174.54 | 185.89 | 34.85 | 33.35 | 49.06 | 20.16 | 39.40 | 51.03 |
| CV (%) | 5.33 | 7.70 | 8.40 | 1.42 | 4.32 | 2.21 | 4.03 | 8.62 | 3.87 | 6.87 | 6.37 | 4.99 | 32.37 | 27.58 | 9.43 | 9.63 | 44.59 | 15.88 | 18.96 | 38.18 |

CV, coefficient of variation.

differences between Operators A and C, A and D and B and D for CBCT Case 3; and for all the operators except A and C for CBCT Case 4.

There were significant differences between the operators in all cases except Case 3 for the edge-based with anisotropic filter procedure (ANOVA). The *post hoc* test showed significant differences between A and D, B and D and C and D for Case 2; B and C and B and D for Case 4; A and C and B and C for Case 5; and between all the operators except between A and D for Case 1 (Table 2).

*Comparison between protocols*

In cases where the operators agreed with each other, a comparison was made with an unpaired *t*-test. In the other cases, the difference between operators forcibly led to a difference of segmentation between manual and semi-automatic protocols.

Cases 1 and 5 had comparable results between the manual and edge-based procedures (non-significant difference). In Case 5, the result could be explained by the existence of an important dispersion in the measures, making this particular result unreliable.

The comparison between the manual and region competition procedures showed non-significant differences in three cases (1, 2 and 5). For Case 5, the conclusion is the same as before. Cases 1 and 2 had no cortical bone destruction, unlike the three other cases.

For all cases, results of the EBDA procedure were significantly different from those of manual segmentation. This technique does not allow accurate semi-automatic segmentation as it did not provide reproducible results.

## Discussion

The aim of this study was to test and compare a manual segmentation protocol with three active contour segmentations for the delineation of dento-maxillary osteolytic lesions. The manual protocol was validated as a reference in our study. The objective was to develop a semi-automatic protocol comparable to the manual procedure with an acceptable coefficient of variation and no statistically significant difference regarding lesion volume for all cases tested. The present investigation produced mixed results. For the semi-automatic procedures, region competition segmentation had the least operator effect and gave the best results. This procedure was comparable to manual segmentation for the lesion without destruction of the cortical bone. The EBDA procedure had the largest operator effect and did not provide reproducible results. The semi-automatic protocol tested here was interesting but was not usable in all cases. These methods were not repeatable and remained unreliable in complex cases. All parameters need to be improved. A post-treatment would be necessary in most of our test cases. Edge-based segmentation methods, which use local edge information to evolve the contour of edges, fail at boundaries where the edges between the

ROI and background are not sharp or clear. Region-based segmentation methods use different intensity distributions of the ROI and background to separate them. These methods fail in areas where the region inside the ROI has similar intensity levels to those of the background.[19] In these periradicular lesions, bone resorption was not uniform. There were many variations in their shape, their size, their extension and their intensity distribution. The boundaries of such lesions can be circumscribed, sharp (Cases 1 and 2) or, conversely, anarchical and non-homogeneous (Case 5). The cortical bone can be blown or broken over a portion of the lesion (Cases 3 and 4).

The tested procedures are a good basis for work, but it is essential to develop a tool more suited to this type of pathology. Hybrid segmentation protocols could overcome these limitations and problems.[19,20] Despite this, it is likely that a manual post-treatment will always be necessary, in cases where cortical bone is broken or there are few sharp or clear boundaries, to remove the overflow generated by the semi-automatic protocol, even when optimized.

One recent study examined an innovative tool, a 3D smart brush, which seems to provide a reliable and fast method of segmentation in odontogenic cyst and tumour surgery, although this study was performed on MSCT rather than CBCT.[21] Several studies have been performed on CBCT in order to evaluate and optimize the segmentation step for the head and neck region, including condyle,[22] and teeth and jaws.[23,24] However, to our knowledge, no studies have yet been performed on CBCT and odontogenic cysts.

In the present investigation, five CBCT image data sets were used. The selected scans had a 200-μm resolution, which was the common resolution proposed by our equipment for $4 \times 5$ or $7 \times 5$ cm fields of view with normal settings. This is a compromise between the noise and possibilities of image processing. The high-resolution settings, proposed by our CBCT device, lead to high noise in the images that, at present, prevent accurate segmentation. CBCT has been described to visualize high contrast structures such as bone in a comparable way to conventional CT. The level of radiation exposure is lower, and the metal artefacts are reduced.[25] CBCT with a limited volume is well suited for the diagnosis of periapical pathology, as used in planning for endodontic surgery.[3,26,27] Limited volume CBCT provides images at high spatial resolution, with low radiation doses and displaying accurate measurements.[26,28]

Its disadvantage is the lack of tissue information.[25] Segmentation in CBCT is often more complex because the image is noisier than in MSCT, owing to lower bone signal-to-noise ratio. The image contrast between the tooth root and the alveolar bone is lower in CBCT. The tooth boundary is too ambiguous to be exactly defined.[19]

The contrast, signal-to-noise ratio and sharpness of the images obtained from CBCT acquisitions still need to be improved to make the segmentation easier.[29] The initial image quality is very important. Parameter variations lead to significant differences in image quality. This influences the potential to visualize the structures that need to be analysed. The voxel size, acquisition quality, accurate resolution and limited noise need to be adapted to the clinical situation. The image must provide information in adequate quantity to allow a sufficient degree of certainty when making a decision. *In vivo* conditions impose some settings that affect image quality. Indeed, acquisition time must be as short as possible to limit radiation exposure. However, it is CBCT scan time and voxel size that are the main factors influencing jawbone model accuracy.[30] Scans of real patients contain more artefacts and reduction in spatial resolution owing to natural micro-movements of the jaw.

CBCT has somewhat lower segmentation accuracy than MSCT; but, considering the results obtained with low radiation, the short scanning time and good image quality, CBCT could be helpful for surgery in the orofacial region.[31]

ITK-SNAP software was chosen because it was developed for the treatment of medical images. Therefore, active contours ("snakes") were adapted for our investigation. It was validated for segmentation of brain MRI images.[14] It is also a free open source software: anybody can use it and can modify the source code to adapt and optimize the segmentation algorithm to their needs.

Semi-automatic segmentation methods are user-guided. The work requires a manual element and guidance, consisting of fast and accurate refinement techniques to assist the human operator.[13] Computation time for the semi-automatic processing was less than 10 min compared with the manual procedure, which took >1 h.

Image segmentation is a fundamental problem in image analysis. The segmentation procedure gives the surgeon information about the total volume and dimensions of a lesion and the spatial relationship between the lesion and any high-risk structure in its proximity. It is a helpful additional process in preoperative diagnosis.[8]

The accuracy of segmentation relies on the grey value and threshold value defined by the operator. Periradicular cyst variability and the frequent absence of a strong grey gradient near their boundaries make the segmentation step difficult, which leads to an overextension of the segmentation beyond the limits of the lesion with the semi-automatic procedure. Owing to the lack of distinctive features that can describe the boundary of the lesions, it is difficult to achieve segmentation with a high degree of accuracy. This leads to underestimation or overestimation of size. It is hard to segment accurately, even using the manual procedure, when visual features (boundaries, regions etc.) are not sufficiently dense, robust or discriminating. Each procedure requires some degree of compromise.

To limit these problems, segmentation requires a thorough knowledge of the images to be analysed and of the information to be extracted subsequently. A good knowledge of the situation enables the user to separate artefacts and noise from what is of interest. The subjectivity involved in this method can lead to different

results being found by two users or by a single user between two segmentations of the same tooth. Prior training of users in displaying the segmentation of the images before starting is interesting[29] and should be considered. In our study, half of the operators were not highly trained for the segmentation protocols to be tested. The aim was to determine if these protocols can be applied by a novice or a non-expert. In any case, subjective ability of the observers must also be taken into account.

In the medical field, it seems to be impossible for a segmentation algorithm to meet all the requirements owing to the large numbers of characteristic differences between organs and tissues.[32]

Manual post-processing, which benefits from the skilled eye and judgment of a clinician, is still required to rectify the semi-automatic procedure. The problem this approach poses is that it usually takes longer (up to several hours) and is therefore not practical.

Segmentation is not easy and its complexity is not often taken into account.[33] Nevertheless, high-quality segmentation within CBCT images of patients requiring oral surgery is a prerequisite for surgical planning, simulation and guidance. Likewise, image quality of CBCT is a prerequisite for accurate segmentation. The CT scanners have excellent spatial accuracy, but their quality needs to be improved in terms of signal-to-noise ratio, contrast and measurement of the radiodensity. Acquisition parameters have to be correctly chosen by the clinician. The CBCT manufacturers also should optimize the technical characteristics of their products to obtain better quality CT scans.

Research on advanced segmentation methods is essential to obtain a semi-automatic accurate individual segmentation of dento-maxillary osteolytic lesions and their environments.[11]

The present study has contributed to testing some semi-automatic segmentation protocols on dento-maxillary imaging. Further investigations need to be performed in order to improve segmentation quality.

## Conclusion

Region-based active contour segmentation was comparable to the manual procedure for delineating circumscribed osteolytic dento-maxillary lesions. However, region-based and boundary-based segmentations are not suitable for all cases. These approaches are limited when segmenting objects with complex surface structures. A hybrid methodology, combining both manual and semi-automatic protocols, needs to be developed in order to provide a suitable method for the majority of cases, regardless of clinical situation, extent and position of the lesion.

The improvement of the image analysis must be considered both through the segmentation procedure and through CBCT image quality (limited noise, augmented contrast etc.).

### Acknowledgments

The authors would like to thank Dr Vincent Morin, Associate Professor, for his statistical help.

### References

1. Pohlenz P, Blessmann M, Blake F, Heinrich S, Schmelzle R, Heiland M. Clinical indications and perspectives for intraoperative cone-beam computed tomography in oral and maxillofacial surgery. *Oral Surg Oral Med Oral Pathol Oral Radiol Endod* 2007; **103**: 412–17. doi: 10.1016/j.tripleo.2006.05.008
2. Liang X, Jacobs R, Hassan B, Li L, Pauwels R, Corpas L, et al. A comparative evaluation of cone beam computed tomography (CBCT) and multi-slice CT (MSCT) part I. On subjective image quality. *Eur J Radiol* 2010; **75**: 265–9. doi: 10.1016/j.ejrad.2009.03.042
3. Patel S, Durack C, Abella F, Shemesh H, Roig M, Lemberg K. Cone beam computed tomography in endodontics—a review. *Int Endod J* 2015; **48**: 3–15. doi: 10.1111/iej.12270
4. Ludlow JB, Laster WS, See M, Bailey LJ, Hershey HG. Accuracy of measurements of mandibular anatomy in cone beam computed tomography images. *Oral Surg Oral Med Oral Pathol Oral Radiol Endod* 2007; **103**: 534–42. doi: 10.1016/j.tripleo.2006.04.008
5. Lascala CA, Panella J, Marques MM. Analysis of the accuracy of linear measurements obtained by cone beam computed tomography (CBCT-NewTom). *Dentomaxillofac Radiol* 2004; **33**: 291–4. doi: 10.1259/dmfr/25500850
6. Brown J, Jacobs R, Levring Jäghagen E, Lindh C, Baksi G, Schulze D, et al; European Academy of DentoMaxilloFacial Radiology. Basic training requirements for the use of dental CBCT by dentists: a position paper prepared by the European Academy of DentoMaxilloFacial Radiology. *Dentomaxillofac Radiol* 2014; **43**: 20130291. doi: 10.1259/dmfr.20130291
7. Estrela C, Bueno MR, Azevedo BC, Azevedo JR, Pécora JD. A new periapical index based on cone beam computed tomography. *J Endod* 2008; **34**: 1325–31. doi: 10.1016/j.joen.2008.08.013
8. Stoetzer M, Nickel F, Rana M, Lemound J, Wenzel D, von See C, et al. Advances in assessing the volume of odontogenic cysts and tumors in the mandible: a retrospective clinical trial. *Head Face Med* 2013; **9**: 14. doi: 10.1186/1746-160X-9-14
9. Koivisto T, Bowles WR, Rohrer M. Frequency and distribution of radiolucent jaw lesions: a retrospective analysis of 9,723 cases. *J Endod* 2012; **38**: 729–32. doi: 10.1016/j.joen.2012.02.028
10. Pak JG, Fayazi S, White SN. Prevalence of periapical radiolucency and root canal treatment: a systematic review of cross-sectional studies. *J Endod* 2012; **38**: 1170–6. doi: 10.1016/j.joen.2012.05.023
11. Cevidanes LH, Tucker S, Styner M, Kim H, Chapuis J, Reyes M, et al. Three-dimensional surgical simulation. *Am J Orthod Dentofacial Orthop* 2010; **138**: 361–71. doi: 10.1016/j.ajodo.2009.08.026
12. Esposito SA, Huybrechts B, Slagmolen P, Cotti E, Coucke W, Pauwels R, et al. A novel method to estimate the volume of bone defects using cone-beam computed tomography: an *in vitro* study. *J Endod* 2013; **39**: 1111–15. doi: 10.1016/j.joen.2013.04.017
13. Suetens P, Bellon E, Vandermeulen D, Smet M, Marchal G, Nuyts J, et al. Image segmentation: methods and applications in diagnostic radiology and nuclear medicine. *Eur J Radiol* 1993; **17**: 14–21. doi: 10.1016/0720-048X(93)90023-G

14. Yushkevich PA, Piven J, Hazlett HC, Smith RG, Ho S, Gee JC, et al. User-guided 3D active contour segmentation of anatomical structures: significantly improved efficiency and reliability. *Neuroimage* 2006; **31**: 1116–28. doi: 10.1016/j.neuroimage.2006.01.015
15. Caselles V, Kimmel R, Sapiro G. Geodesic active contours. *Int J Comput Vis* 1997; **22**: 61–79. doi: 10.1023/A:1007979827043
16. Zhu S-C, Yuille A. Region competition: unifying snakes, region growing, and Bayes/MDL for multiband image segmentation. *IEEE Trans Pattern Anal Mach Intell* 1996; **18**: 884–900.
17. Weissheimer A, Menezes LM, Sameshima GT, Enciso R, Pham J, Grauer D. Imaging software accuracy for 3-dimensional analysis of the upper airway. *Am J Orthod Dentofacial Orthop* 2012; **142**: 801–13. doi: 10.1016/j.ajodo.2012.07.015
18. Itksnap.org. [Cited 4 March 2015]. Available from: http://www.itksnap.org/pmwiki/pmwiki.php?n=Main.HomePage
19. Ji DX, Ong SH, Foong KW. A level-set based approach for anterior teeth segmentation in cone beam computed tomography images. *Comput Biol Med* 2014; **50**: 116–28. doi: 10.1016/j.compbiomed.2014.04.006
20. Chen T, Metaxas D. A hybrid framework for 3D medical image segmentation. *Med Image Anal* 2005; **9**: 547–65. doi: 10.1016/j.media.2005.04.004
21. Rana M, Modrow D, Keuchel J, Chui C, Rana M, Wagner M, et al. Development and evaluation of an automatic tumor segmentation tool: a comparison between automatic, semi-automatic and manual segmentation of mandibular odontogenic cysts and tumors. *J Craniomaxillofac Surg* 2015; **43**: 355–9. doi: 10.1016/j.jcms.2014.12.005
22. Xi T, Schreurs R, Heerink WJ, Bergé SJ, Maal TJ. A novel region-growing based semi-automatic segmentation protocol for three-dimensional condylar reconstruction using cone beam computed tomography (CBCT). *PLoS One* 2014; **9**: e111126. doi: 10.1371/journal.pone.0111126
23. Gan Y, Xia Z, Xiong J, Zhao Q, Hu Y, Zhang J. Toward accurate tooth segmentation from computed tomography images using a hybrid level set model. *Med Phys* 2015; **42**: 14–27. doi: 10.1118/1.4901521
24. Naumovich SS, Naumovich SA, Goncharenko VG. Three-dimensional reconstruction of teeth and jaws based on segmentation of CT images using watershed transformation. *Dentomaxillofac Radiol* 2015; **44**: 20140313. doi: 10.1259/dmfr.20140313
25. Schulze D, Heiland M, Blake F, Rother U, Schmelzle R. Evaluation of quality of reformatted images from two cone-beam computed tomographic systems. *J Craniomaxillofac Surg* 2005; **33**: 19–23.
26. Lofthag-Hansen S, Huumonen S, Gröndahl K, Gröndahl H-G. Limited cone-beam CT and intraoral radiography for the diagnosis of periapical pathology. *Oral Surg Oral Med Oral Pathol Oral Radiol Endod* 2007; **103**: 114–19. doi: 10.1016/j.tripleo.2006.01.001
27. Hassan B, Couto Souza P, Jacobs R, de Azambuja Berti S, van der Stelt P. Influence of scanning and reconstruction parameters on quality of three-dimensional surface models of the dental arches from cone beam computed tomography. *Clin Oral Investig* 2010; **14**: 303–10. doi: 10.1007/s00784-009-0291-3
28. Lofthag-Hansen S, Thilander-Klang A, Gröndahl K. Evaluation of subjective image quality in relation to diagnostic task for cone beam computed tomography with different fields of view. *Eur J Radiol* 2011; **80**: 483–8. doi: 10.1016/j.ejrad.2010.09.018
29. Maret D, Telmon N, Peters OA, Lepage B, Treil J, Inglèse JM, et al. Effect of voxel size on the accuracy of 3D reconstructions with cone beam CT. *Dentomaxillofacial Radiol* 2012; **41**: 649–55. doi: 10.1259/dmfr/81804525
30. Vandenberghe B, Luchsinger S, Hostens J, Dhoore E, Jacobs R; SEDENTEXCT Project Consortium. The influence of exposure parameters on jawbone model accuracy using cone beam CT and multislice CT. *Dentomaxillofac Radiol* 2012; **41**: 466–74. doi: 10.1259/dmfr/81272805
31. Liang X, Lambrichts I, Sun Y, Denis K, Hassan B, Li L, et al. A comparative evaluation of cone beam computed tomography (CBCT) and multi-slice CT (MSCT). Part II: on 3D model accuracy. *Eur J Radiol* 2010; **75**: 270–4. doi: 10.1016/j.ejrad.2009.04.016
32. Yau HT, Yang TJ, Chen YC. Tooth model reconstruction based upon data fusion for orthodontic treatment simulation. *Comput Biol Med* 2014; **48**: 8–16. doi: 10.1016/j.compbiomed.2014.02.001
33. Michetti J, Maret D, Mallet JP, Diemer F. Validation of cone beam computed tomography as a tool to explore root canal anatomy. *J Endod* 2010; **36**: 1187–90. doi: 10.1016/j.joen.2010.03.029